

AD-A062 014

AEROSPACE CORP EL SEGUNDO CALIF IVAN A GETTING LABS F/G 14/2
DOUBLE MICHELSON INTERFEROMETER FOR CONTACTLESS LENGTH CHANGE M--ETC(U)
NOV 78 E G WOLFF, S A ESELUN F04701-78-C-0079
TR-0079(4950-01)-1 SAMSO-TR-78-136 NL

UNCLASSIFIED

| OF |
AD
A062014



END
DATE
FILMED
3-79
DDC

LEVEL II

12

Double Michelson Interferometer for Contactless Length Change Measurements

E. G. WOLFF and S. A. ESELUN
Materials Sciences Laboratory
The Ivan A. Getting Laboratories
The Aerospace Corporation
El Segundo, Calif. 90245

DDC
RECEIVED
DEC 11 1978
F

6 November 1978

Interim Report

APPROVED FOR PUBLIC RELEASE;
DISTRIBUTION UNLIMITED

Prepared for
SPACE AND MISSILE SYSTEMS ORGANIZATION
AIR FORCE SYSTEMS COMMAND
Los Angeles Air Force Station
P.O. Box 92960, Worldway Postal Center
Los Angeles, Calif. 90009

78 12 04.030

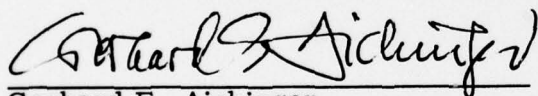
ADA062014

DDC FILE COPY

This interim report was submitted by The Aerospace Corporation, El Segundo, CA 90245, under Contract No. F04701-78-C-0079 with the Space and Missile Systems Organization, Contracts Management Office, P.O. Box 92960, Worldway Postal Center, Los Angeles, CA 90009. It was reviewed and approved for The Aerospace Corporation by W. C. Riley, Director, Material Sciences Laboratory. Gerhard E. Aichinger was the project officer for Mission-Oriented Investigation and Experimentation (MOIE) Programs.

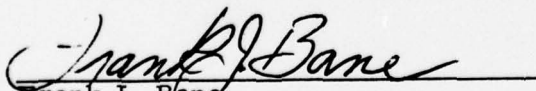
This report has been reviewed by the Information Office (OI) and is releasable to the National Technical Information Service (NTIS). At NTIS, it will be available to the general public, including foreign nations.

This technical report has been reviewed and is approved for publication. Publication of this report does not constitute Air Force approval of the report's findings or conclusions. It is published only for the exchange and stimulation of ideas.



Gerhard E. Aichinger
Project Officer

FOR THE COMMANDER



Frank J. Bane
Chief Contracts Management Office

UNCLASSIFIED

SECURITY CLASSIFICATION OF THIS PAGE (When Data Entered)

19 REPORT DOCUMENTATION PAGE		READ INSTRUCTIONS BEFORE COMPLETING FORM	
1. REPORT NUMBER 18 SAMSO TR-78-136	2. GOVT ACCESSION NO.	3. REPORT'S CATALOG NUMBER 9	
4. TITLE (and Subtitle) 6 DOUBLE MICHELSON INTERFEROMETER FOR CONTACTLESS LENGTH CHANGE MEASUREMENTS		5. TYPE OF REPORT & PERIOD COVERED Interim <i>Rept.</i>	
7. AUTHOR(s) 10 Ernest G. Wolff and Steve A. Eselun		14. PERFORMING ORG. REPORT NUMBER TR-0079(4950-01)-1	15. CONTRACT OR GRANT NUMBER(s) F04701-78-C-0079
9. PERFORMING ORGANIZATION NAME AND ADDRESS The Aerospace Corporation El Segundo, Calif. 90245		10. PROGRAM ELEMENT, PROJECT, TASK AREA & WORK UNIT NUMBERS	
11. CONTROLLING OFFICE NAME AND ADDRESS Space and Missile Systems Organization Air Force Systems Command Los Angeles, Calif. 90009		12. REPORT DATE 11 6 November 1978	
14. MONITORING AGENCY NAME & ADDRESS (if different from Controlling Office) 12 27p.		13. NUMBER OF PAGES 21	
		15. SECURITY CLASS. (of this report) Unclassified	
		15a. DECLASSIFICATION/DOWNGRADING SCHEDULE	
16. DISTRIBUTION STATEMENT (of this Report) Approved for public release; distribution unlimited			
17. DISTRIBUTION STATEMENT (of the abstract entered in Block 20, if different from Report)			
18. SUPPLEMENTARY NOTES			
19. KEY WORDS (Continue on reverse side if necessary and identify by block number) Interferometry Thermal Strains Thermal Expansion Length Measurements Laser Metrology <i>epsilon</i>			
20. ABSTRACT (Continue on reverse side if necessary and identify by block number) The use of a two-channel, or double Michaelson, interferometer for measuring the absolute thermal strain ϵ of a small test sample (e.g., 4-in. long) is described. This method is contactless inasmuch as laser beams reflect off the ends of the sample. Real-time strain changes are recorded automatically to a resolution of $\lambda/8L_s$, where L_s is the sample length. Analysis shows that the measurement errors are approximately proportional to the sample temperature excursion, with the strain error varying from 4.8×10^{-8} to 2×10^{-7} as <i>next page</i> <i>4.8 to 2 x 10 to the -7 power</i>			

DD FORM 1473
(FACSIMILE)

UNCLASSIFIED

SECURITY CLASSIFICATION OF THIS PAGE (When Data Entered)

Lambda

subs

409944

78

12

04-030

7B

UNCLASSIFIED

SECURITY CLASSIFICATION OF THIS PAGE(When Data Entered)

19. KEY WORDS (Continued)

Delta T sub 5

20. ABSTRACT (Continued)

ΔT varies from 25 to 250 C. An average coefficient of thermal expansion for ultralow-expansion glass, measured with additional fringe interpolation by photo-detector signal analysis, would be known to $\pm 1.2 \times 10^{-9} \text{ } ^\circ\text{C}^{-1}$.

+ or - 1.2 times 10 to the -9th power/deg-C

UNCLASSIFIED

SECURITY CLASSIFICATION OF THIS PAGE(When Data Entered)

CONTENTS

I.	INTRODUCTION	3
II.	THEORY OF TWO-CHANNEL INTERFEROMETER	5
III.	EXPERIMENTAL APPARATUS AND PROCEDURE	9
IV.	ERROR ANALYSIS	17
V.	EXPERIMENTAL RESULTS	19
VI.	DISCUSSION	23
APPENDIX: CALCULATION OF STRAIN GRADIENT FOR CYLINDRICAL SPECIMENS FOR GIVEN TEMPERATURE DISTRIBUTIONS		25

FIGURES

1.	Two-Channel Michelson Interferometer	6
2.	Apparatus for Heating Cylindrical Samples	10
3.	Side View of Two-Channel Interferometer	11
4.	Sample Support System for Ultralow Temperature Length Change Measurements	12
5.	Electronic Signal Processing from Two-Channel Interferometer	14
6.	Typical Photodetector Signals on Sample Heating	15
7.	Calibration Data Obtained with NBS-SRM-739 Fused Silica . . .	20



I. INTRODUCTION

The advantages of reflected laser beams for the measurement of dimensions in changing thermal environments have been documented.^{1, 2} The use of interferometric techniques for these measurements results in the elimination of dependence on a reference material. The laser frequency can be readily known and stabilized, through use of the Lamb dip, to one part in 10^9 in 500 hr.¹ When all the optics are placed in the test (vacuum) chamber, there is no possible error from refraction in beam paths, window effects, or operators, since all information is generated at the beam splitter(s).

A Michelson interferometer was originally used in The Aerospace Corporation Materials Sciences Laboratory (MSL) to study length changes of samples heated to ± 250 C.¹ In this case, one arm of the interferometer included both ends of the test sample, which resulted in a large optical path length (OPL) difference between the two beams required to recombine in order to form the necessary fringe pattern. An extensive analysis indicated that there are several possible sources of error inherent in this approach.¹ Because the OPL of the sample was so much greater (70 times) than that to the reference mirror, errors could arise as a result of differences in pressure or temperature of the residual gas in the two OPLs. More importantly, because all the optics used in the sample OPL were held on the same support plate, any temperature changes in any part of this plate would change the sample OPL, which the interferometer would then confuse with a sample length change. In principle, this error could be avoided by a zero coefficient of thermal expansion (CTE) support plate. This would be approximated by

¹E. G. Wolff and S. A. Eselun, Absolute Length Changes by Remote Interferometry, TR-0076(6950-07)-1, The Aerospace Corp., El Segundo, Calif. (10 December 1975).

²E. G. Wolff, "Measurement Techniques for Low Expansion Materials, Nat. SAMPE Tech. Conf. Ser. 9, 57 (1977).

ultralow-expansion glass (ULE) near room temperature ($\text{CTE} \sim 0 \pm 0.03 \times 10^{-6} \text{ }^{\circ}\text{C}^{-1}$). A sufficiently large and stiff plate, however, is extremely expensive (stiffness provides immunity from vacuum chamber distortions on pumpdown or ambient temperature fluctuations). The error might also be avoided by the use of a water-cooled copper baseplate attached to a thermostatically controlled bath. Undesirable vibration could result, however, because the optics would have to be attached rigidly to the plate. Another problem with a one-channel interferometer is that 10 or 11 reflections must be aligned sequentially for recombination with a reference beam.

II. THEORY OF TWO-CHANNEL INTERFEROMETER

The principles of a two-channel Michelson interferometer are illustrated in Fig. 1. The original laser beam (frequency-stabilized He-Ne) is split 50/50 at beam splitter BS3 into right and left (sample) side interferometers. With the sample ends designated S and the mirrors M, it can be seen that, for the right-hand side, the interferometer optical path length difference (OPLD) is

$$\text{OPLD}_1 = \overline{B_1 S_1} - \overline{B_1 M_6} \quad (1)$$

Similarly

$$\text{OPLD}_2 = \overline{B_2 M_5} - \overline{S_2 M_4} - \overline{B_2 M_4} \quad (2)$$

Now

$$\Delta \text{OPLD}_2 - \Delta \text{OPLD}_1 = \overline{\Delta B_2 M_5} - \overline{\Delta S_2 M_4} - \overline{\Delta B_2 M_4} - \overline{\Delta B_1 S_1} + \overline{B_1 M_6} \quad (3)$$

Assume that

$$\overline{\Delta B_2 M_4} = \overline{\Delta B_1 M_6} \quad (a)$$

$$\overline{\Delta B_1 M_4} = \overline{\Delta B_2 M_5} \quad (b)$$

Note that

$$\overline{\Delta B_1 M_4} = \overline{\Delta S_2 M_4} + \Delta L_s + \overline{\Delta S_1 B_1}$$

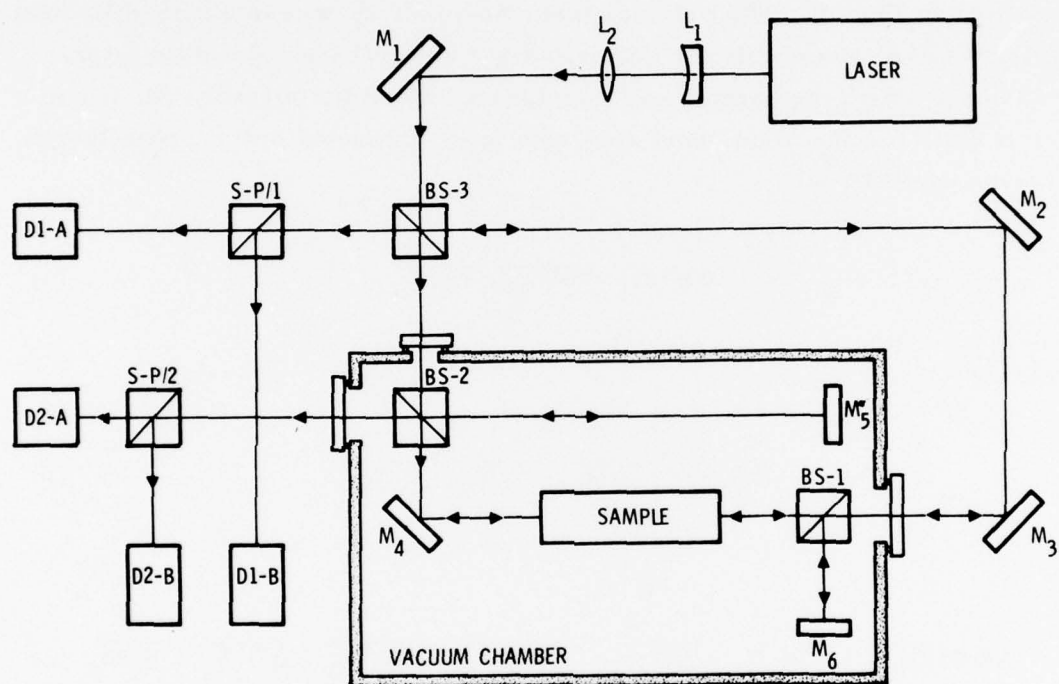


Fig. 1. Two-Channel Michelson Interferometer

where L_s is the sample length. Hence

$$\Delta L_s = \Delta \text{OPLD}_2 - \Delta \text{OPLD}_1 \quad (4)$$

Consequently, the sample length change ΔL_s is merely the difference between the changes in the two OPLDs.

III. EXPERIMENTAL APPARATUS AND PROCEDURE

Three methods studied to support the test sample are illustrated in Figs. 2 through 4. In all cases, the cross section of the material is arbitrary, the length is limited only by the size of the vacuum chamber (and resultant optics separation) available, and the size is limited by the amount of heat flow (again chamber-size limited) the system can tolerate. Another sample support method that was investigated involves the use of axial adjacent quartz rods supported on ULE blocks outside the cooler/heater unit. Expansion was discontinuous, probably because of sample weight-induced friction effects on the support used. The use of thin (~ 0.125 -in. thick) horizontal transverse support rods (usually made of Invar) (Fig. 2), has met with much success, primarily because slight variations in heat flow along the rods have a minimal effect on the position of the sample in space, and the sample supports are approximately room temperature at all times. Temperature changes of the sample support are minimized by placing the support structure (Invar cylinders) far away from the sample (and heat or cold source). The large volume of Invar at the extremities of the $1/8$ -in. cross bars acts as a heat sink; these bars are designed to have low surface/volume ratio for this purpose. The surfaces are also polished to increase reflectance of radiation. Absorbant coatings on the sample help to increase the efficiency of heat transfer to the sample and to minimize heat flow to the supports.

The sample support shown in Fig. 3 was sensitive to small temperature gradients and hence caused sample rotations. High (Cu), medium (Invar), and low (SiO_2) CTE supports were tried. An additional disadvantage of this approach is the conduction of heat to or from the optics support plate. The use of a copper plate to minimize temperature gradients in the optics support plate is also illustrated in Fig. 3. There is need for a zero-CTE (over ± 250 C) material to support the test sample. Plano convex

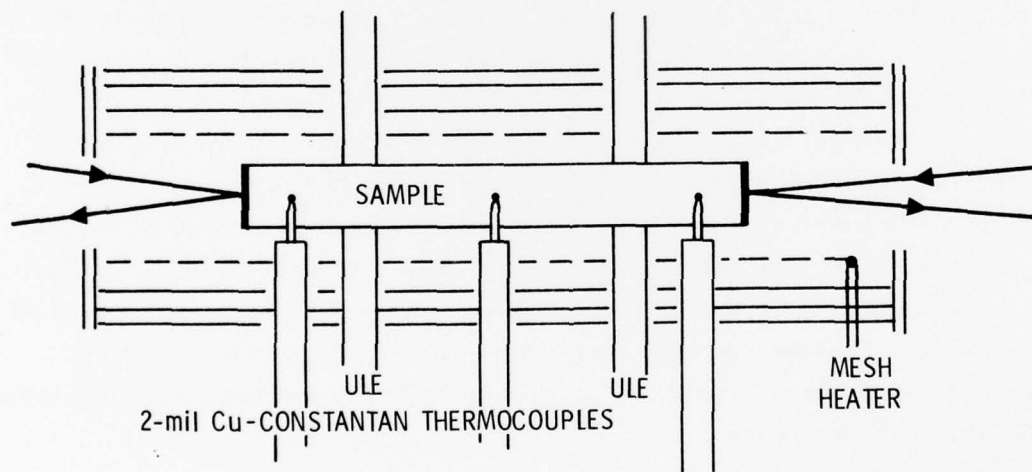
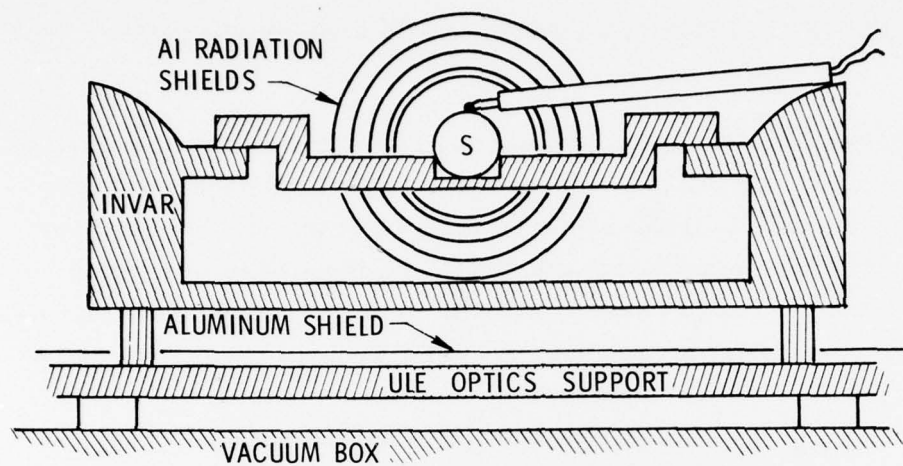


Fig. 2. Apparatus for Heating Cylindrical Samples

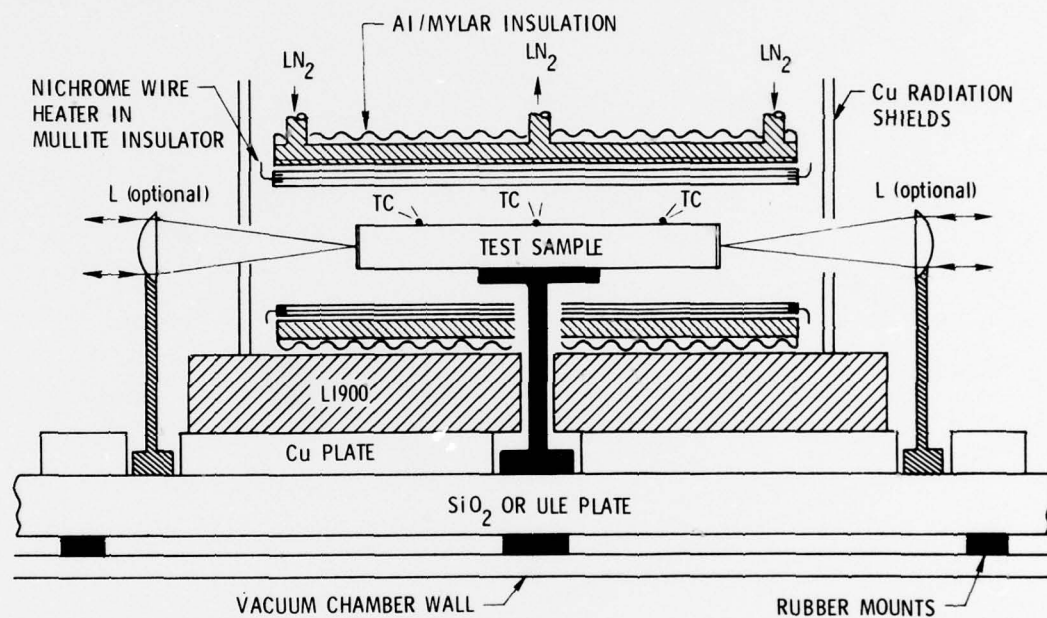


Fig. 3. Side View of Two-Channel Interferometer

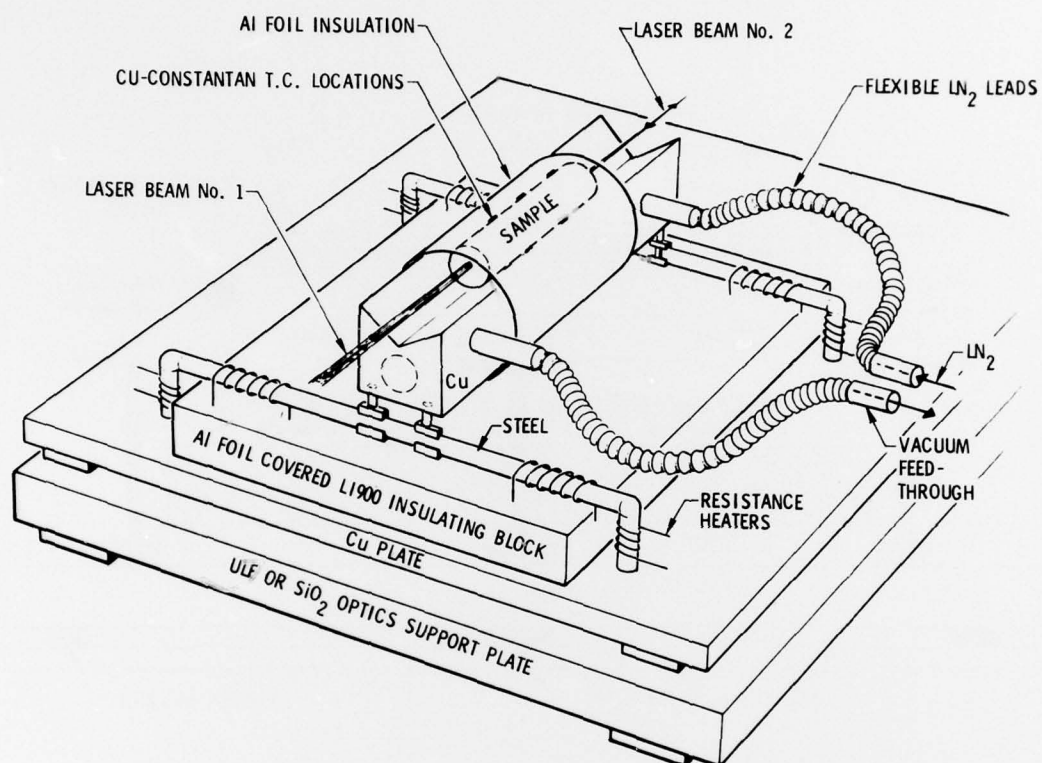


Fig. 4. Sample Support System for Ultralow Temperature Length Change Measurements

focusing lenses* are also used to ensure that the reflected beams recombine with the reference beam in spite of small sample rotations. The system under test for very low temperature work is shown in Fig. 4. The radiation heat transfer method (Figs. 2 and 3) requires very long time periods to achieve temperatures much lower than -100 C. Cooling is a more difficult task than heating, not only because of reduced radiation heat transfer, but also because the required use of liquid N₂ or He imposes greater temperature gradients on the system.

The electronic signal processing used to convert the four photodetector signals to an analog voltage proportional to the sample length change is shown in Fig. 5. The SP beam splitters (SP1 and SP2) separate orthogonal components of the circularly polarized laser beam, an essential feature in detecting the directionality of fringe motion. The clipping circuit then digitizes the resulting silicon photodetector signals. By combining two dependent signals, the logic circuit is able to count the ΔL changes in steps of $\lambda/8$ and strain in steps of $\lambda/8L_0$, which, for a 4-in. sample, equals 7.79×10^{-7} . If required, interpolation can be achieved by recording the original analog voltage (Fig. 6); a 2π phase (δ) change is equivalent to $\lambda/2$ and

$$V(\text{signal}) = V_{DC} + V_{AC} \cos \delta \quad (7)$$

With this technique, δ can be obtained to high resolution.¹ In general, however, system vibration and noise (which are phase dependent, as shown in Fig. 6) limit the sensitivity to $\lambda/1000$ - $\lambda/100$.

*E. G. Wolff and S. A. Eselun, "Thermal Expansion of a Fused Quartz Tube in a Dimensional Stability Test Facility," Rev. Sci. Instrum. (to be published, 1978).

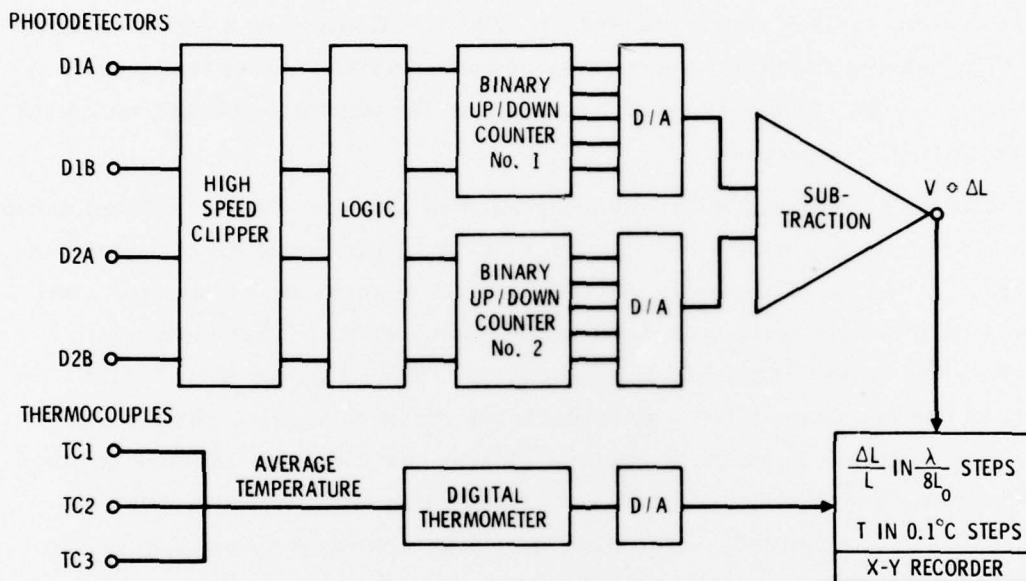


Fig. 5. Electronic Signal Processing from Two-Channel Interferometer

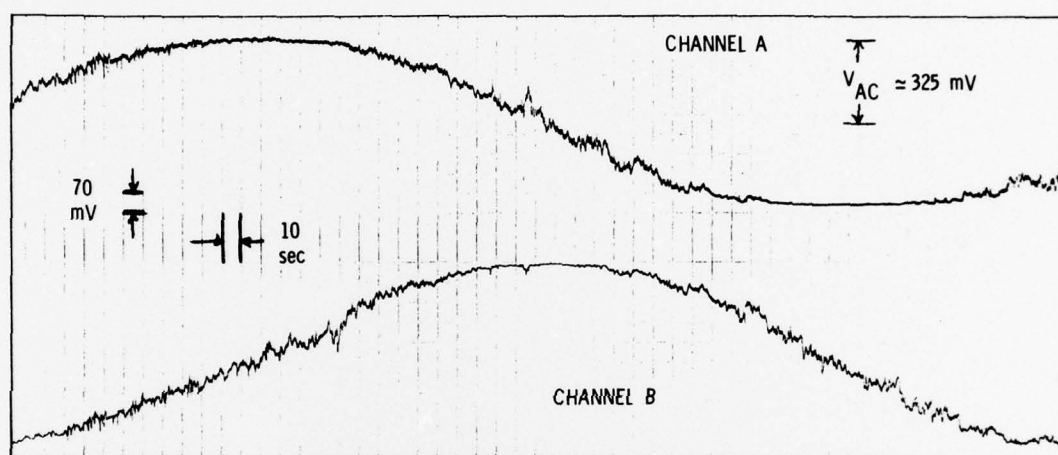


Fig. 6. Typical Photodetector Signals on Sample Heating

IV. ERROR ANALYSIS

The accuracy of the system, Eq. (4), depends on the validity of the assumptions (a) and (b). The combination of distance from the test sample and symmetry ensures that assumption (a) is incorrect by only a small amount, because the temperature difference between these regions is small (≤ 0.3 C). Hence,

$$\Delta E_1 = \alpha \overline{B_2 M_4} \Delta T = (3 \times 10^{-8}) (2) (0.3) = 1.8 \times 10^{-8} \text{ in.} \quad (8)$$

The strain error in a 4-in. sample then is 4.5×10^{-9} .

Assumption (b) is similarly incorrect, but the low CTE support plate ULE compensates for the greater significant length (20 in.) and somewhat higher temperature differentials. The copper plate (Figs. 3 and 4) is used to reduce temperature gradients to ≤ 1 C at the test temperature extremes. Hence,

$$\Delta E_2 = \alpha \overline{B_2 M_5} \Delta T = (3 \times 10^{-8}) (20) (1) \leq 6 \times 10^{-7} \text{ in.} \quad (9)$$

and, for a 4-in. sample, the strain error is $\leq 1.5 \times 10^{-7}$.

Besides the design errors discussed above, problems may arise as a result of shifting of the sample ends relative to the laser beams and because of temperature gradients within the sample. Sample support rotations must be minimized in order to avoid signal loss. In practice, such losses occur before errors caused by off-axis beam reflectance become significant. Mere translation of the reflecting surface would not result in measurement errors if the end faces are parallel to each other and perpendicular to the sample axis. If there is a small angle γ between the end planes, and

shrinkage of support posts occurs, an error is induced even without sample expansion or contraction. It can be readily shown that this error is

$$\Delta E_3 = l_s \alpha_s \Delta T \gamma \quad (10)$$

where s refers to the support material in the direction perpendicular to the laser beam axis. For 1/8-in.-thick Invar supports (Fig. 2) and γ of 1 deg, ΔE_3 for ΔT of 250 C is 5.45×10^{-7} in.; angle γ can be ~ 8 deg before the strain error exceeds 1 $\mu\epsilon$ on a 4-in.-long test sample at the temperature extremes.

Thermal strain errors may arise if large (radial) temperature gradients are set up in the sample as a result of rapid heating or cooling. In the Appendix, it is shown that the length change error will be

$$\Delta E_4 = L_s \Delta \epsilon = \frac{\alpha L_s (1 + \nu) (T_s - T_c)}{2(1 - 2\nu)} \quad (11)$$

where ν is the Poisson's ratio, and T_s and T_c are the surface ($r = R$) and center ($r = 0$) temperatures, respectively. It can be shown that, for times equal to or greater than R^2/a , where a is the thermal diffusivity, the gradient $T_s - T_c$ remains constant at

$$T_s - T_c \approx \frac{1}{4} \frac{dT}{dt} \frac{R^2}{a} \quad (12)$$

A 4-in. fused silica rod of 1/4-in. diam can achieve a steady gradient in about 12 sec ($= R^2/a$). If $\nu = 0.17$, $dT/dt \sim 5$ C/min (0.083 C/s), $\Delta E_4 \sim 4.4 \times 10^{-7}$ in. This error will decrease for higher thermal conductivity materials and slower rates.

V. EXPERIMENTAL RESULTS

The data in Fig. 7 were obtained from several tests of the NBS-SRM 739 fused silica standard ($l_0 = 3.35$ in.), which was polished and lightly coated at the ends with a thin film of aluminum for reflectance. The scatter band is well within the NBS standard deviation of $\pm 6 \times 10^{-6}$ in/in $\Delta L/L$. Some of the data obtained during these tests from reading two bidirectional counters (I_1, I_2) and a digital readout of the average temperature are given in Table 1. Since the three individual thermocouple readings were not read simultaneously, only their range about the average is indicated. This range decreases with higher conductivity materials.

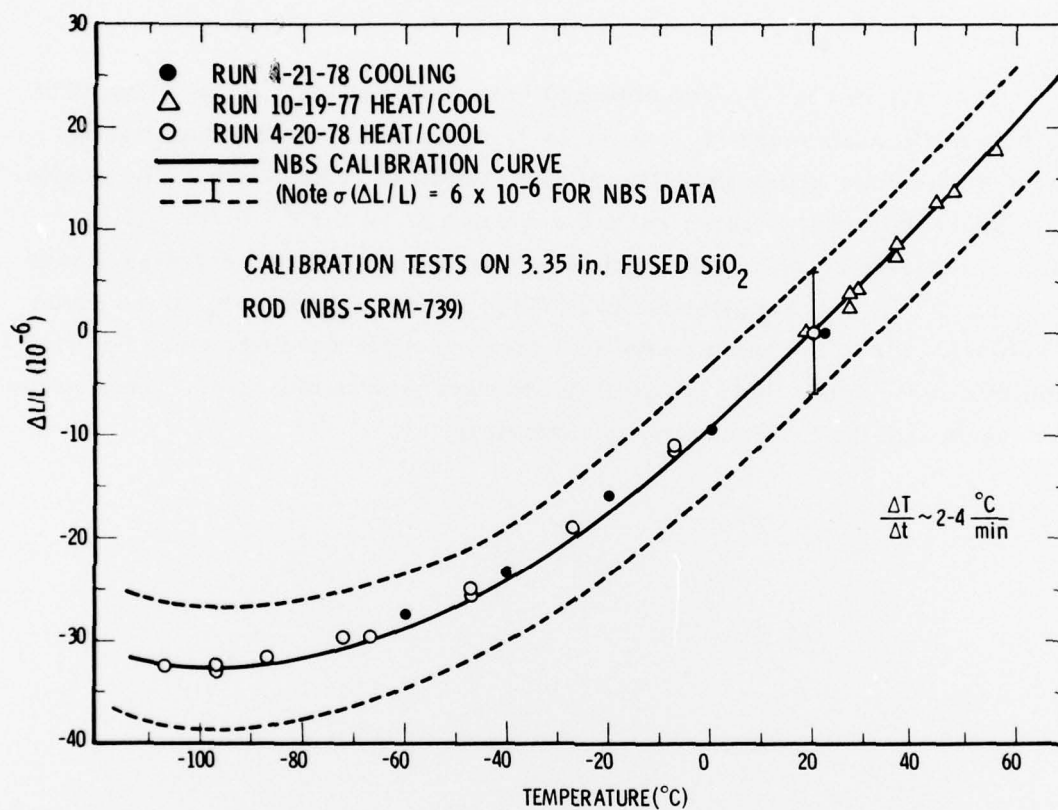


Fig. 7. Calibration Data Obtained with NBS-SRM-739 Fused Silica

Table 1. Typical Data Sheet for Sample Fused SiO_2 (SRM 739)^a

Time 4/20/78	T_{AV}, K	T_{AV}, C	\dot{T} range, K	I_1	I_2	$I_2 - I_1$	$\Delta L/L, \times 10^{-6}$ ^b
1:15	300	27	0	0	0	0	0
1:36	273	0	2	10	-2.5	-12.5	-11.6
1:41	263	-10	2	14	-2	-16	-14.8
1:45	253	-20	2.5	16	-3.5	-19.5	-18.1
1:50	233	-40	3	21.5	-6	-27.5	-25.5
1:55	208	-65	4	24	-7.5	-31.5	-29.2
2:00	183	-90	4.5	23	-12	-35	-32.5
2:08	153	-120	5	12	-22	-34	-31.6
2:14	143	-130	4	7	-25	-32	-29.7
2:27	153	-120	5	2	-29	-31	-28.8
2:41	183	-90	6	14	-22	-36	-33.4
2:54	213	-60	7	12	-20	-32	-29.7
3:01	233	-40	5	9	-18	-27	-25.1
3:28	300	27	5	10	-10	0	0

^aNBS-SRM-739 uses $T_o = 20 C$, not 27 C shown here.

^b $\Delta L/L = \lambda/8L_o (I_2 - I_1)$

VI. DISCUSSION

The interferometric technique may be refined by the use of thermoelectric cooling elements for complex-shaped samples. These elements are thermodynamically inefficient, however, and heat dissipation could cause problems. Thermal positioning actuators are being studied by means of the ultralow-temperature apparatus (Fig. 4). Results of preliminary tests indicate that slight sample rotations can be corrected by heating a sample support post. The use of a piezoelectric crystal attached to the M_6 mirror (Fig. 1) may also improve the technique. Electronic control to maintain $\Delta S_1 B_1 = \Delta B_1 M_6$ means that $\Delta L_s = \Delta OPLD_2$ only, and that only one detection channel is required.

The most serious problem has involved signal losses that resulted from slight support rotations at the extreme temperatures and excessive time required to achieve very low temperatures. The ultralow-temperature apparatus (Fig. 4) is expected to correct these two remaining problems, neither of which affects measurement accuracy.

The sensitivity or resolution of the automatic recording system is $\lambda/8$ (791 Å, 3.11 μ in. or 7.78×10^{-7} strain on a 4-in. sample). Fringe interpolation could be used to reduce these figures by a factor of about 100. The accuracy of these measurements, however (in principle, a measure of their traceability to a standard), is affected by thermal gradients in the system and by sample end face geometry. The former errors are approximately proportional to the sample temperature excursion, and thus the total strain values are more accurate at 0 or 50 C than at ± 250 C. With all ULE optics supports, $\gamma = 1$ deg and $dT/dt = 2$ C/min, the sum of all errors for a 250 C excursion equals 3.34×10^{-7} strain, equivalent to an rms strain error of 2.07×10^{-7} in a 4-in. sample. At 0 or 50 C, the latter figure diminishes to $\sigma_e = 4.8 \times 10^{-8}$. An average CTE measurement on ULE

(where $\epsilon = +60 \mu\epsilon$ at -200 C) implies an rms error σ_{CTE} of $1.2 \times 10^{-9} \text{ }^{\circ}\text{C}^{-1}$. The error in ΔT measurement is 0.7 C because it depends on temperature difference between two thermocouples that have an absolute accuracy of only about $\pm 0.5 \text{ C}$. Fringe interpolation would be needed in order to realize this accuracy in CTE inasmuch as the resolution of the automatic system is slightly greater than σ_{ϵ} . The automatic system could then determine the CTE to $\pm 3.5 \times 10^{-9} \text{ }^{\circ}\text{C}^{-1}$.

APPENDIX

CALCULATION OF STRAIN GRADIENT FOR CYLINDRICAL SPECIMENS FOR GIVEN TEMPERATURE DISTRIBUTIONS

With the surface temperature defined as

$$T_s = T_o + kt$$

where $k = \Delta T / \Delta t$, upon reaching steady state

$$T = T_o + kt - \frac{k}{4a} (R^2 - r^2)$$

and

$$T = T_o + kt - \frac{kR^2}{8a}$$

where a is the thermal diffusivity. Under plane strain conditions

$$\sigma_{zz} = \frac{\alpha E}{1 - 2\nu} \left[\frac{2}{R^2} \int_0^R T r \, dr - T \right]$$

$$\sigma_{zz} = \frac{\alpha E}{1 - 2\nu} [\bar{T} - T]$$

But

$$\epsilon_{zz} = \alpha T + \frac{(1 - \nu)}{E} \sigma_{zz}$$

$$\epsilon_{zz} = \frac{\alpha}{1-2\nu} (1-\nu) T - \nu T$$

$$\epsilon_{zz} = \alpha T_s - \frac{\alpha k R^2}{(1-2\nu) 8a} \left[1 + \nu + \frac{2\nu r^2}{R^2} \right]$$

and since the measurement is made at $r = 0$,

$$\Delta \epsilon = \frac{\alpha(T_s - T_c)(1+\nu)}{2(1-2\nu)}$$

THE IVAN A. GETTING LABORATORIES

The Laboratory Operations of The Aerospace Corporation is conducting experimental and theoretical investigations necessary for the evaluation and application of scientific advances to new military concepts and systems. Versatility and flexibility have been developed to a high degree by the laboratory personnel in dealing with the many problems encountered in the nation's rapidly developing space and missile systems. Expertise in the latest scientific developments is vital to the accomplishment of tasks related to these problems. The laboratories that contribute to this research are:

Aerophysics Laboratory: Launch and reentry aerodynamics, heat transfer, reentry physics, chemical kinetics, structural mechanics, flight dynamics, atmospheric pollution, and high-power gas lasers.

Chemistry and Physics Laboratory: Atmospheric reactions and atmospheric optics, chemical reactions in polluted atmospheres, chemical reactions of excited species in rocket plumes, chemical thermodynamics, plasma and laser-induced reactions, laser chemistry, propulsion chemistry, space vacuum and radiation effects on materials, lubrication and surface phenomena, photosensitive materials and sensors, high precision laser ranging, and the application of physics and chemistry to problems of law enforcement and biomedicine.

Electronics Research Laboratory: Electromagnetic theory, devices, and propagation phenomena, including plasma electromagnetics; quantum electronics, lasers, and electro-optics; communication sciences, applied electronics, semiconducting, superconducting, and crystal device physics, optical and acoustical imaging; atmospheric pollution; millimeter wave and far-infrared technology.

Materials Sciences Laboratory: Development of new materials; metal matrix composites and new forms of carbon; test and evaluation of graphite and ceramics in reentry; spacecraft materials and electronic components in nuclear weapons environment; application of fracture mechanics to stress corrosion and fatigue-induced fractures in structural metals.

Space Sciences Laboratory: Atmospheric and ionospheric physics, radiation from the atmosphere, density and composition of the atmosphere, aurorae and airglow; magnetospheric physics, cosmic rays, generation and propagation of plasma waves in the magnetosphere; solar physics, studies of solar magnetic fields; space astronomy, x-ray astronomy; the effects of nuclear explosions, magnetic storms, and solar activity on the earth's atmosphere, ionosphere, and magnetosphere; the effects of optical, electromagnetic, and particulate radiations in space on space systems.

THE AEROSPACE CORPORATION
El Segundo, California